VII Brazilian Symposium on Rock Mechanics – SBMR 2016
Rock Mechanics and Rock Engineering for Innovation and Development
ISRM Specialized Conference 19-22 October, Belo Horizonte, Minas Gerais, Brazil

Analytical solution for the stability analysis of rock slopes against block toppling failure subjected to seismic loads

Congxin Chen
State Key Laboratory of Geomechanics and Geotechnical Engineering, Institute of Rock and Soil Mechanics, Chinese Academy of Sciences, Wuhan, Hubei 430071, China
Email: cxchen@whrsm.ac.cn

Yun Zheng*
State Key Laboratory of Geomechanics and Geotechnical Engineering, Institute of Rock and Soil Mechanics, Chinese Academy of Sciences, Wuhan, Hubei 430071, China
Email: zhengyun19332009@126.com

Haina Zhang
State Key Laboratory of Geomechanics and Geotechnical Engineering, Institute of Rock and Soil Mechanics, Chinese Academy of Sciences, Wuhan, Hubei 430071, China
Email: hainawisdom@163.com

SUMMARY: Toppling is a typical failure mode of rock slopes dominantly controlled by the discontinuities existing in the slopes, which are often encountered in constructions of various geotechnical engineering. This failure has been classified into two principal types, namely block toppling and flexural toppling. This paper concentrates on the former. To provide a guiding significance for the engineering design, the analysis of rock anti-inclined slopes against block toppling failure due to seismic loads is conducted. On the basis of the limit equilibrium method, a general analytical solution of block toppling failure subjected to seismic loads is deduced for the cases that the block slenderness ratio is relatively large. Furthermore, the explicit expressions are given for the conditions when the geometry is simple. Using the analytical solution, the magnitude of the inter-column forces, the location of failure mode transition point and the magnitude of the toe residual sliding force can be determined. Through four typical examples, the effects of seismic loads on the failure mode of rock anti-inclined slopes, the maximum allowable of the line normal to dip for block toppling failure to occur, and the location of failure mode transition point. The results show that the failure mode of rock anti-inclined slopes can be changed by seismic loads, with the increase of the earthquake influence coefficient, the failure mode is gradually changed from the toppling-sliding failure to the overall sliding failure; The maximum normal angle of the steep discontinuities for block toppling failure to occur and the earthquake influence coefficient have direct negative correlation; with increasing the earthquake influence coefficient, the location of failure mode transition point gradually moves on the latter and the range of the sliding toe gradually expands when the toppling-sliding failure occurs.

KEYWORDS: Rock anti-inclined slopes, Block toppling failure, the limit equilibrium method, Seismic loads.

1 INTRODUCTION

Toppling failure mainly exists in layered rock mass with steep dip angle, which often appears at the dig face near the slope's surface (Yang et al. 2006). Many scholars devote to study the causes, failure modes and reinforcement measures of toppling failure and have achieved remarkable results. This failure has been classified into two principal types, namely block toppling and flexural toppling. This paper concentrates on the former.

On the basis of the limit equilibrium method, Goodman and Bray (1976) proposed the step by step analysis method, establishing the theoretical foundation for the stability analysis of rock slopes against block toppling failure. Later, many scholars have developed this method (Zanbak C. 1983; Aydan et al. 1989; Kliche CA. 1999; Liu et al. 2008a, 2009; Lu et al. 2012). Meanwhile, numerical methods, such as manifold method and discrete element, have also been used to analyze the toppling failure and obtained achievements. For the block slenderness is relatively large, the number of block need to be analyzed would be high, which is time consuming and error-prone if the calculations are carried out manually. Aimed at this problem, A. Bobet (1999) proposed the continuum method to analyze block toppling failure. Assuming the base line is normal to the dip of the dominant discontinuities, he deduced the limit equilibrium differential equation and analytical solution for the stability analysis of rock slopes against block toppling failure. Later, Sagaseta et al (2001) and Liu et al (2008b) extended the continuum solution to more complex cases. The results show that the continuum method has sufficient accuracy when the block slenderness ratio is greater than 20-30.

Previous studies mainly focus on the stability analysis of rock slopes against block toppling failure under gravity. Nevertheless, few scholars study the mechanism of block toppling failure for rock slopes under seismic load. Thus, an innovative approach has been proposed in this paper for the stability analysis of rock slopes against block toppling failure under seismic load.

2 CONTINUUM APPROACH

2.1 General assumptions

When the spacing of discontinuities t decreases indefinitely, the blocks transform into differential slices of width $\mathrm{d}x$ (Sagaseta et al. 2001), as shown in Figure 1. Thus, the equilibrium equations in the Goodman and Bray (1976) lead to ordinary differential equations that can be easily integrated in the case that rock slopes subjected to seismic load.

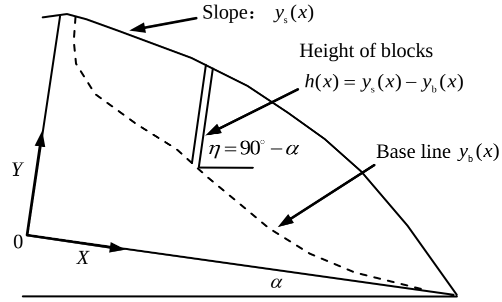

Figure 1. Geometry of slope

As shown in Figure. 1, the slope surface and the base line can have any irregular shape, defined by $y_s(x)$ and $y_b(x)$, respectively. The block height $h(x) = y_s(x) - y_b(x)$. α is inclination of the line normal to dip; η is the dip angle of the dominant discontinuities. In any case, the base of each block is always normal to dip. The axes OX and OY are taken normal and parallel to dip.

The two basic assumptions proposed by Goodman and Bray (1976) were still used in this paper, as follows:

(1) The limit friction equilibrium condition is satisfied along the interface of adjacent rock columns.

(2) The total side force is assumed to be acted at the top of the rock interface.

2.2 Mechanical model

Based on the above assumptions, the mechanical model of each block against block toppling failure under seismic load is shown in Figure 2.

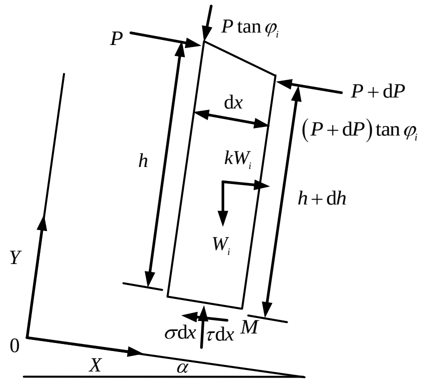

Figure 2. Mechanical model of each block against block toppling failure under seismic load

For column i, the moment equilibrium equation can be expressed as

$$(P+\mathrm{d}P)(h+\mathrm{d}h)\text{-}P[h+(-\frac{\mathrm{d}y_b}{\mathrm{d}x})\mathrm{d}x]+P\tan\varphi_i\mathrm{d}x = (W_i\sin\alpha+kW_i\cos\alpha)\frac{h}{2}+(kW_i\sin\alpha-W_i\cos\alpha)\frac{\mathrm{d}x}{2} \quad (1)$$

Where P and $P+\mathrm{d}P$ are normal force on the left and righ sides, respectively; h is the block height; φ_i is friction angle between bedding planes; k is the seismic influence coefficient; The weight of column i can be expressed as :

$$W_i = \gamma h \mathrm{d}x \quad (2)$$

Where γ is the unit weight of the rock mass.Omitting the high order infinitesimal, Equation (1) can be simplified as

$$\frac{\mathrm{d}P}{\mathrm{d}x}+\frac{1}{h}(\frac{\mathrm{d}y_s}{\mathrm{d}x}+\tan\varphi_i)P=\frac{1}{2}\gamma h\sin\alpha+\frac{1}{2}k\gamma h\cos\alpha \quad (3)$$

At the limit rotational balance condition, the normal stress σ and shear stress τ, can be , respectively , expressed as

$$\begin{aligned}\sigma &= \gamma h\cos\alpha-\frac{\mathrm{d}P}{\mathrm{d}x}\tan\varphi_i-k\gamma h\sin\alpha\\ \tau &= \gamma h\sin\alpha-\frac{\mathrm{d}P}{\mathrm{d}x}+k\gamma h\cos\alpha\end{aligned} \quad (4)$$

The limit sliding balance equation for block, under the seismic load can be expressed as

$$\frac{\mathrm{d}P}{\mathrm{d}x}=-\gamma h\cos\alpha A_s+k\gamma h\cos\alpha A_g \quad (5)$$

At the limit sliding balance condition, σ and τ , can be , respectively , expressed as

$$\begin{aligned}\sigma &= \gamma h\cos\alpha A_k-k\gamma h\cos\alpha A_h\\ \tau &= \gamma h\cos\alpha\tan\varphi_b A_k-k\gamma h\cos\alpha\tan\varphi_b A_h\end{aligned} \quad (6)$$

Where

$$\begin{aligned}A_s &= \frac{\tan\varphi_b-\tan\alpha}{1-\tan\varphi_b\tan\varphi_i};A_g=\frac{1+\tan\alpha\tan\varphi_b}{1-\tan\varphi_b\tan\varphi_i}\\ A_k &= \frac{1-\tan\alpha\tan\varphi_i}{1-\tan\varphi_b\tan\varphi_i};A_h=\frac{\tan\alpha+\tan\varphi_i}{1-\tan\varphi_b\tan\varphi_i}\end{aligned} \quad (7)$$

Where φ_b is the friction angle along transverse joints.

2.3 Modes of failure

If the toppling failure mode is applied, the shear stress at the block base cannot exceed its shear strength and tensile stress should not appear either, expressed as Equation (8). Otherwise, the sliding failure mode should be used.

$$\sigma \geqslant 0, \frac{\tau}{\sigma} \leqslant \tan\varphi_b \quad (8)$$

3 BASIC CASE

3.1 Geometric model

The method is applied to the basic case of a slope of height H shown in Figure 3. β_g is the dip angle of the natural ground; β is the dip angle of the cut slope; θ is the plunge of the base line. The following auxiliary parameters are defined to simplify the analyses that follow:

$$\begin{cases}\psi=\beta-\alpha\\ \omega=\beta_g-\alpha\\ \xi=\theta-\alpha\end{cases} \quad (9)$$

Expressions for the shapes of the slope surface and the base line can be, respectively, written as:

$$y_s(x) = \begin{cases} -\tan\omega x + \tan\xi L & x \leqslant x_B \\ \tan\psi(L - x) & x > x_B \end{cases} \tag{10}$$

$$y_b = \tan\xi\left(L - x\right) \tag{11}$$

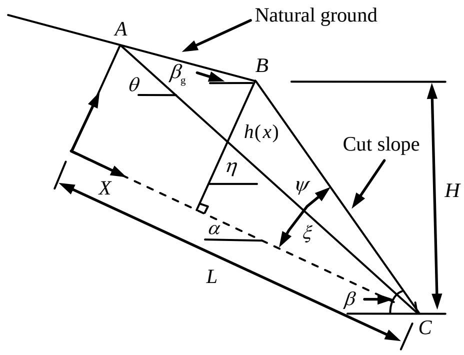

Figure 3. Typical slope geometry of toppling failure

It can be seen from Figure 3 that the heights of block below and above the crest are expressed, respectively, as:

$$h(x) = \begin{cases} -\left(\tan\omega - \tan\xi\right)x & x \leqslant x_B \\ \left(\tan\psi - \tan\xi\right)(L - x) & x > x_B \end{cases} \tag{12}$$

To simplify the analyses, the following auxiliary parameters are defined:

$$\left.\begin{aligned} \tan\psi' &= \tan\psi - \tan\xi \\ \tan\omega' &= \tan\omega - \tan\xi \\ \tan\varphi_i' &= \tan\varphi_i - \tan\xi \\ \tan\varphi_b' &= \tan\varphi_b - \tan\xi \end{aligned}\right\} \tag{13}$$

3.2 Analytical solution

The integration starts from point A with $P = 0$ for $x = 0$. Unlike the finite block analysis, there is no stable zone, because the blocks of infinitesimal width can never be stable against toppling except on a horizontal base (Sagaseta et al. 2001). For the case of toppling, the solution in the region AB is:

$$P = \frac{1}{2}\gamma(\sin\alpha + k\cos\alpha)\frac{\tan^2\omega'}{\tan\varphi_i' - 3\tan\omega'}x^2 \tag{14}$$

Then, by putting formula (14) into (4), the σ and τ at the base, can be, respectively, expressed as

$$\left.\begin{aligned} &\sigma = -\gamma\tan\omega'\cos\alpha\left(1 + \frac{\tan\alpha\tan\varphi_i\tan\omega'}{\tan\varphi_i' - 3\tan\omega'}\right)x + \\ &k\gamma\tan\omega'\cos\alpha\left(\tan\alpha - \frac{\tan\varphi_i\tan\omega'}{\tan\varphi_i' - 3\tan\omega'}\right)x \\ &\tau = -\gamma\tan\omega'\sin\alpha\left(1 + \frac{\tan\omega'}{\tan\varphi_i' - 3\tan\omega'}\right)x + \\ &k\gamma\tan\omega'\cos\alpha\left(1 + \frac{\tan\omega'}{\tan\varphi_i' - 3\tan\omega'}\right)x \end{aligned}\right\} \tag{15}$$

According to the condition (8), k and α should meet the following inequalities, if the toppling failure mode is applied.

$$\left.\begin{aligned} &k\tan\alpha - 1 \leqslant \frac{\tan\varphi_i\tan\omega'}{\tan\varphi_i' - 3\tan\omega'}(\tan\alpha + k) \\ &\tan\alpha - \tan\varphi_b + k(1 + \tan\alpha\tan\varphi_b) \leqslant \\ &-\tan\omega'\frac{1 - \tan\varphi_b\tan\varphi_i}{\tan\varphi_i' - 3\tan\omega'}(\tan\alpha + k) \end{aligned}\right\} \tag{16}$$

If these conditions are not satisfied, sliding occurs. Then the whole wedge ABC slides and the solution is trivial, which would not be discussed in this paper.

The normal force the solution in the region BC is:

$$\begin{aligned} P = {} & \frac{1}{2}\gamma(\sin\alpha + k\cos\alpha)\frac{\tan^2\psi'}{\tan\varphi_i' - 3\tan\psi'}(L - x_B)^2 \cdot \\ & \left[\left(\frac{L - x}{L - x_B}\right)^2 - 3\frac{\tan\psi' - \tan\omega'}{\tan\varphi_i' - 3\tan\omega'}\left(\frac{L - x}{L - x_B}\right)^{\frac{\tan\varphi_i'}{\tan\psi'} - 1}\right] \end{aligned} \tag{17}$$

Then, by putting formula (12) into (4), the normal stress σ and shear stress τ at the base in the region BC, can be, respectively, expressed as:

$$\left.\begin{aligned}\sigma &= \gamma\cos\alpha\tan\psi'(L-x)-\frac{\mathrm{d}P}{\mathrm{d}x}\tan\varphi_i- \\ &\quad k\gamma\sin\alpha\tan\psi'(L-x) \\ \tau &= \gamma\sin\alpha\tan\psi'(L-x)-\frac{\mathrm{d}P}{\mathrm{d}x}+k\gamma\cos\alpha\tan\psi'(L-x)\end{aligned}\right\} \quad (18)$$

As discussed in previous studies (Sagaseta et al. 2001; Liu et al. 2008b), if toppling occurs down slope to the slope toe under seismic load, equation 17 indicates that the support force at the toe will be infinite $\psi>\varphi_i$ when and zero when $\psi<\varphi_i$. In other words, the slope will be unstable when $\psi>\varphi_i$, however, will always be maintained in a state of limite quilibrium when $\psi<\varphi_i$. In practice, it is impossible for these situations to occur. Therefore, there must exist a point x_T, where the slope failure mode transform from block toppling failure into sliding failure. Three cases with $\psi<\varphi_i$, $\psi>\varphi_i$, and $\psi=\varphi_i$ are presented below.

3.2.1 Case one ($\psi<\varphi_i$)

It can be seen from Figure 4 that σ decreases first and then increases with increasing x when $\psi<\varphi_i$. τ almost no change with x before the curve $\sigma-x$ and curve $\tau-x$ intersect. Between the crest and the intersection, there exists a point x_T that the shear stress at the block base reaches the shear strength, as expressed:

$$\tau=\sigma\tan\varphi_{\mathrm{b}} \quad (19)$$

Eq. 20 can be obtained by Eqs. 17, 18, and 19.

$$\left(\frac{L-x_{\mathrm{T}}}{L-x_B}\right)^{\frac{\tan\varphi_i'}{\tan\psi'}-3}=\frac{2}{3}\frac{(\tan\varphi_i'-3\tan\omega')\tan\psi'}{(\tan\psi'-\tan\omega')(\tan\varphi_i'-\tan\psi')}\cdot \left[1+\frac{3\tan\psi'-\tan\varphi_i'}{\tan\psi'(k+\tan\alpha)}\left(A_{\mathrm{s}}-kA_{\mathrm{g}}\right)\right] \quad (20)$$

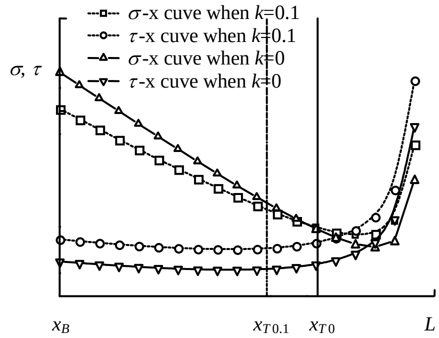

Figure 4. Curves of σ vs x and τ vs x (ψ <φ i)

The block toppling failure occurs before x_T while the sliding failure occurs after x_T, which forms sliding slope toe. This failure mode is called ST. Without considering the seismic load, namely $k=0$, the curves $\sigma-x$ and $\tau-x$ are in accordance with previous studies (Sagaseta et al. 2001; Liu et al. 2008b)，as is shown in Figure 4, which proves the derivation of the analytical expression is correct in this paper.

When $k=0.1$, the slope failure mode doesn't change, but the transition point changes form x_{T0} to $x_{T0.1}$, indicating the scope of sliding front has widened. Due to the seismic load, the normal stress at the block base decreases and the shear stress increases at the same time, reducing the base anti-sliding force and increasing the sliding force, making intersection move backward and the scope of sliding slope toe larger.

For the region below the transition point x_T, sliding failure occurs. The sliding force P can be obtained by integrating Eq. 5

$$P=P_T-\frac{1}{2}\gamma\cos\alpha\tan\psi' A_{\mathrm{s}}\left[\left(L-x_T\right)^2-\left(L-x\right)^2\right] +\frac{1}{2}k\gamma\cos\alpha\tan\psi' A_g\left[\left(L-x_T\right)^2-\left(L-x\right)^2\right] \quad (21)$$

Where P_T can be obtained by Eqs. 17 and 20. The mechanical model of sliding slope toe is shown as Figure 5.

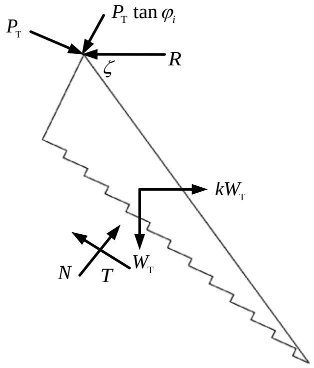

Figure 5. Mechanical model of sliding slope toe

The reinforced force required to maintain slope stability can be expressed as

$$R=\frac{1}{\cos\left(\zeta-\psi\right)+\sin\left(\zeta-\psi\right)\tan\varphi_{\mathrm{b}}}\cdot \left[P_{\mathrm{T}}\left(1-\tan\varphi_i\tan\varphi_{\mathrm{b}}\right)+ W_{\mathrm{T}}\left(\sin\alpha-\cos\alpha\tan\varphi_{\mathrm{b}}\right)+ kW_{\mathrm{T}}\left(\cos\alpha+\sin\alpha\tan\varphi_{\mathrm{b}}\right)\right] \tag{22}$$

Where W_T is the weight of sliding slope toe; ζ is the angle between the reinforced force and the cut slope.

In addition, the residual sliding force can be also obtained from Eq. 21

$$P_{\mathrm{S}}=P_{\mathrm{T}}-\frac{1}{2}\gamma\cos\alpha\tan\psi' A_{\mathrm{s}}\left(L-x_{\mathrm{T}}\right)^2+ \frac{1}{2}k\gamma\cos\alpha\tan\psi' A_{\mathrm{g}}\left(L-x_{\mathrm{T}}\right)^2 \tag{23}$$

Therefore, according to the toe residual sliding force, the reinforced force can be also expressed as:

$$R=\frac{P_{\mathrm{S}}}{\cos\left(\zeta-\psi\right)+\sin\left(\zeta-\psi\right)\tan\varphi_{\mathrm{b}}} \tag{24}$$

3.2.2 Case2 ($\psi>\varphi_i$)

When $\psi>\varphi_i$, there is a point x_T in the region BC where the normal stress σ at the block base is zero, which is the transition point from toppling failure to sliding failure. This failure mode is called TT. Simultaneous solution of Eqs. 17 and 18, x_T can be obtained by Eq. 25.

$$\left(\frac{L-x_{\mathrm{T}}}{L-x_B}\right)^{\frac{\tan\varphi_i'}{\tan\psi'}-3}=\frac{2}{3}\frac{(\tan\varphi_i'-3\tan\omega')\tan\psi'}{(\tan\psi'-\tan\omega')(\tan\varphi_i'-3\tan\psi')}\cdot \left[\left(1-k\tan\alpha\right)-\frac{3\tan\psi'-\tan\varphi_i'}{(k+\tan\alpha)\tan\psi'\tan\varphi_i}\right] \tag{25}$$

When P_T is obtained in equation (17) by x_T, then the reinforced force can also be gotten by Eq. 22 or 24. Without considering the seismic load, namely $k=0$, the curves $\sigma-x$ and $\tau-x$ are in accordance with previous studies (Sagaseta et al. 2001; Liu et al. 2008b), as shown in Figure. 6, which proves the derivation of the analytical expression is correct in this paper. Compared with the case without considering the seismic load, the transition point of failure mode moves backward when $k=0.1$. The influence of k is much smaller compared with that for failure mode ST. The curves $\sigma-x$ and $\tau-x$ are nearly the same for $k=0$ and $k=0.1$.

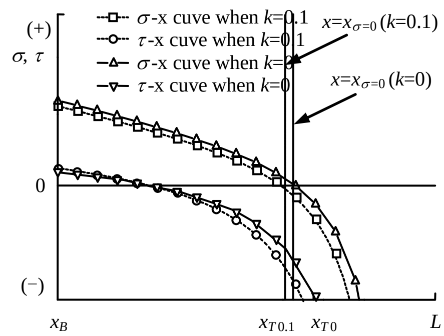

Figure 6. Curves of σ vs x and τ vs x (ψ >φ i)

3.2.3 Case3 ($\psi=\varphi_i$)

When $\psi=\varphi_i$, with the increase of x, both σ and τ linearly decrease and are equal to 0 at the point $x=L$, namely $x_T=L$, shown in Figure. 7. Then, the sliding normal force P_T can be obtained by Eq. 17.

$$P_{\mathrm{T}}=-\frac{3}{2}\gamma(\sin\alpha+k\cos\alpha)\frac{\tan^2\psi'}{\tan\varphi_i'-3\tan\psi'}\cdot \frac{\tan\psi'-\tan\omega'}{\tan\varphi_i'-3\tan\omega'}(L-x_B)^2 \tag{26}$$

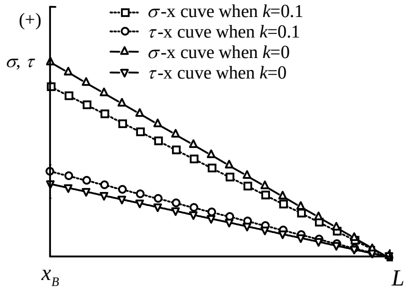

Figure 7. Curves of σ vs x andτ vs x (ψ =φ i)

4 CASE ANALYSIS

The above explores the analytical solution of block toppling failure for rock slopes under seismic load. And the following four examples from previous articles will be used to analyze the effect of the seismic influence coefficient k on the maximum allowable of the line normal to dip for block toppling failure $\alpha_{\max}$ and the failure mode transition point x_T . The calculation parameters are shown in table 1.

4.1 Influence of k on $\alpha_{\max}$

According to Eq. 16, the relation of maximum allowable of the line normal to dip $\alpha_{\max}$ vs seismic influence coefficient k when the block toppling failure occurs can be obtained, as shown in Figure 8. When $0<\alpha<\alpha_{\max}$, the slope may occur block toppling-sliding failure ($\psi \neq \varphi_i$) or pure block toppling failure ($\psi=\varphi_i$). When $\alpha_{\max}<\alpha<90°$, the slope may occur overall sliding failure. From the results of four examples, the relationship of $\alpha_{\max}$ and k is negative correlation. The larger k is, the wider the range of the sliding failure region, indicating that the seismic load can change the slope failure mode from toppling failure to overall sliding failure.

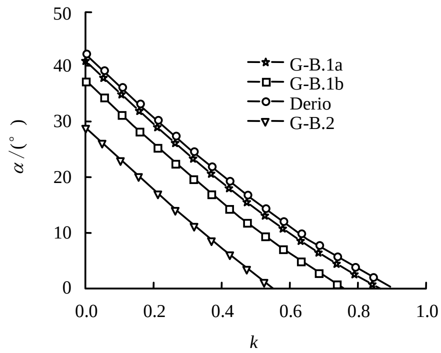

Figure 8. Curves of seismic influence coefficient vs maximum allowable inclinations of the line normal to dip

4.2 Influence of k on x_T

For the convenience of analysis, the sliding proportional coefficient is introduced.

$$\chi=\frac{L-x_{\mathrm{T}}}{L-x_B} \tag{27}$$

Figure 9 shows the relationship of seismic influence coefficient k vs the sliding proportional coefficient χ

According to the relative magnitude of ψ and φ_i, we can know that the failure mode of G-B.1a and G-B.1b are ST, whereas the failure mode of Derio and G-B.2 are TT. With the increase of k , χ increases gradually regardless of ST or TT failure modes (Figure 9), indicating that with the increase of seismic influence coefficient, the transition point of failure mode moves forward and the range of sliding toe extends. In addition, the sensibility of χ to k in ST is apparently higher than that in TT, indicating that the seismic influence coefficient has a greater impact on ST type failure mode than TT type.

Table 1. Calculation parameters of examples

Examples	Parameters								
	H/m	t/m	γ/(kN/m^3)	β/(°)	β_g/(°)	α/(°)	θ/(°)	φ_b/(°)	φ_i/(°)
Derio	39.0	1	25	65.0	0	10	35.0	35.00	25.00
G-B.1.a	92.5	10	25	56.6	4	30	35.8	38.15	38.15
G-B.1.b	92.5	10	25	56.6	4	30	35.8	33.00	33.00
G-B.2	105.6	10	25	60.0	0	20	45.0	21.45	21.45

Table 2 Maximum allowable seismic influence coefficient corresponding to examples when toppling failure occurs

examples	G-B.1a	G-B.1b	Derio	G-B.2
k_{max}	0.19	0.12	0.62	0.15

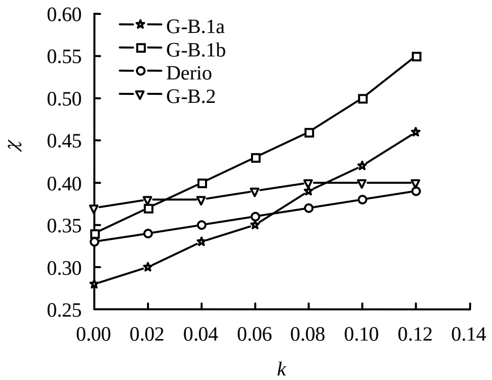

Figure 9. Curves of seismic influence coefficient vs sliding proportional coefficient

5 CONCLUSION

On the basis of the limit equilibrium method, a general analytical solution of block toppling failure subjected to seismic loads is deduced. Furthermore, the explicit expressions are given for the conditions when the geometry is simple, and then case study is conducted. We have drawn four conclusions as follows:

(1) With the increase of seismic influence coefficient, the failure mode of slope maybe changed from toppling-sliding failure to overall sliding failure.

(2) The relationship of α_{max} and k is negative. The bigger of k, the larger range of the sliding toe, while the smaller range of the overall toppling failure.

(3) With increasing the earthquake influence coefficient, the location of failure mode transition point gradually moves on the latter and the range of the sliding toe gradually expands when the toppling-sliding failure occurs.

ACKNOWLEDGEMENTS

We would like to acknowledge the reviewers and the editor for their valuable comments and suggestions. This paper was financially supported by the National Natural Science Foundation of China (Grant No. 11472293)

REFERENCES

Aydan O, Shimizu Y, Ichikawa Y. The effective failure modes and stability of slopes in rock mass with two discontinuity sets[J]. Rock Mechanics and Rock Engineering, 1989, 22(3): 163－88.

Bobet A. Analytical solutions for toppling failure[J]. International Journal of Rock Mechanics and Mining Sciences, 1999, 36(7): 971－980.

Goodman R E, Bray J W. Toppling of rock slopes[C]//Proceedings of ASCE Specialty Conference. Rock Engineering for Foundations and Slopes. Colorado: Boulder, 1976: 201－234.

Kliche CA. Rock slope stability[M]. Colombia: Society for Mining, Metallurgy, and Exploration(SME), 1999.

Liu C H, Jaksa M B, Meyers A G. A transfer coefficient method for rock slope toppling[J]. Canadian Geotechnical Journal, 2009, 46(1): 1－9.

Liu C H, Jaksa M B, Meyers A G. Toppling mechanisms of rock slopes considering stabilization from the underlying rock mass[J]. International Journal of Rock Mechanics and Mining Sciences, 2008a, 45(8): 348－354.

Liu C H, Jaksa M B, Meyers A G. Improved analytical solution for toppling stability analysis of rock slopes[J]. International Journal of Rock Mechanics and Mining Sciences, 2008b, 45(8): 1361－1372.

Lu Hai-feng, Liu Quan-sheng, Chen Cong-xin. Improvement of cantilever beam limit equilibrium model of counter-tilt rock slopes[J]. Rock and Soil Mechanics, 2012, 33(2): 577－584.

Sagaseta C, Sanchez JM, Canizal J. A general analytical solution for the required anchor force in rock slopes with toppling failure[J]. International Journal of Rock Mechanics and Mining Sciences, 2001, 38(3): 421－435.

Yang Gen-lan, Huang Run-qiong, Yan Ming, et al. Engineering geological study on a large-scale topping deformation at xiaowan hydropower station[J]. Journal of Engineering Geology, 2006, 14(2): 165－171.

Zanbak C. Design charts for rock slopes susceptible to toppling[J]. Journal of Geotechnical Engineering, 1983, 109(8): 1039－1062.